12 Laser Dynamics

S. Dangel, H. Neff, R. Holzner

Besides the laser related projects described in the section on surface physics in the group of Prof. Osterwalder, the other main part of our research activities is the investigation of nonlinear spatio-temporal effects caused by the interaction of resonant laser beams with sodium atoms in the gas phase. A circularly polarized laser beam propagating through sodium vapor can optically pump sodium atoms into a nonabsorbing ground state (optical pumping). This strongly nonlinear mechanism which occurs even at very low light intensities causes an intensity dependent refractive index gradient along as well as transverse to the laser beam propagation direction which may give rise to a number of nonlinear spatio-temporal intensity and polarization pattern creating processes. Examples [1, 2] are self-focusing and defocusing of laser beams, beam bouncing [2], beam switching [3], beam splitting [4], processes which transform incident Gaussian beam intensity profiles into ring profiles [5] or the deflection of a laser beam by the inhomogeneous magnetic field of an electric current carrying wire [6]. The numerical simulations for these effects have mainly been done on the SX-3 and SX-4 NEC supercomputers and were also used to produce video animations on a Silicon Graphics Machine with the kind support of Angelo Mangili from the Swiss Scientific Computing Center CSCS in Manno.

For the theoretical description of these effects a number of models have been developed which vary in complexity according to their aims. They have been optimized with regard to simplicity, treatability with analytical tools, inclusion of magnetic field effects, inclusion of the polarization properties of light or many other effects such as optical pumping, radiation trapping or population trapping.

Probably the first and simplest model to describe light-atom interactions is the oscillating dipole model. By assuming an electron in the Coulomb potential of a positive charge driven by the oscillating electric field of a light wave this entirely classical model is capable of describing absorption and dispersion effects which are coupled by the Kramers-Kronig relation and expressed by the imaginary and real part of a complex refractive index. The linewidth of the atomic transition, an intrinsic quantum mechanical quantity, is interpreted as the damping of the oscillation and the binding potential determines the resonance oscillation frequency. From this model one can extract Beer's law for linear absorption in the weak signal approximation. However, it fails for stronger radiation fields since in a real atom saturation occurs.

Saturation is taken into account by the optical Bloch equations [7] which represent the simplest semiclassical model where the light is a classical scalar wave and the atom is treated as a two state quantum mechanical system using a 2×2 density matrix. This treatment is not-perturbative. Since the terms of all orders in the electric field are retained it remains correct even for large field amplitudes. A comparison [7] between the full QED treatment of the atom-radiation interaction with the semiclassical approximation shows that the latter is a good approximation as long as the driving light beam is coherent.

If effects due to the polarization of the electromagnetic radiation should be described, the model for the atom must include the discrimination between the different angular momenta of the atomic states. In the case of the sodium atom a 2-level 4-state semiclassical model known as the $J = 1/2 \leftrightarrow J = 1/2$ model (or short $J_{\frac{1}{2}}$ model) is appropriate for the explanation of many effects. A general treatment of such a model has been given by Ducloy [8] based on irreducible tensors [9, 10]. The model has been further developed for our specific case by McCord and Ballagh in 1990 [11], however, for steady state only. A one-pass system (not containing a cavity) is assumed. An arbitrary intensity and polarization pattern can be taken as input and its propagation through sodium vapor is then calculated numerically. The model includes diffraction, saturation and optical pumping induced polarization effects. As shown in fig.12.1(top) optical pumping by circularly polarized light rearranges the initially equal populations of both ground states in such a way that the medium becomes transparent to the laser beam and all atoms populate the nonabsorbing ground state.

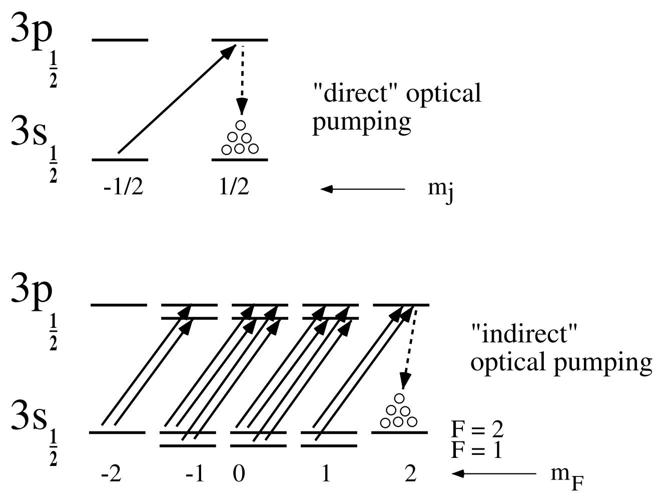

Figure 12.1: Schematic representation of the sodium D_1 atomic transition. Top: neglecting the hyperfine structure leaves only 4 states ($J = 1/2 \leftrightarrow J = 1/2$ model). Optical pumping can occur directly between the $m_j = -\frac{1}{2}$ and $m_j = +\frac{1}{2}$ states. Bottom: full model with all hyperfine levels. Optical pumping occurs in several steps and is about an order of magnitude slower than in the $J = 1/2 \leftrightarrow J = 1/2$ model. Relaxations other than the one to the pumped state are not shown.

Although the $J_{\frac{1}{2}}$ model describes most of the observed behavior qualitatively correct, it often fails to reproduce the true experimentally measured parameter values. It clearly fails e.g. to account for a realistic description of the dynamics of optical pumping related phenomena. In the model the time scale of optical pumping is about one order of magnitude too fast compared to experimental observations [12, 3]. Furthermore, the decay rate of the ground state magnetization due to diffusion has to be adjusted for good agreement between experiment and theory for the laser beam absorption.

Also in the case of external magnetic fields one has to vary the g-factor of the lower level between $\frac{1}{2}$ and 2, depending on the observed effects, to match experimental observations. These shortcomings are overcome by the inclusion of all hyperfine states of the $3S_{1/2}$ and $3P_{1/2}$ energy levels. In fig.12.2 numerical simulations based on models of incresing complexity are compared with observations of a beam switching experiment where optical pumping provides a time delay for the transmitted light. The hyper fine(HF) model is most accurate both with regard to the delay and rise time as well as with regard to the amount of the transmitted light. Some aspects of

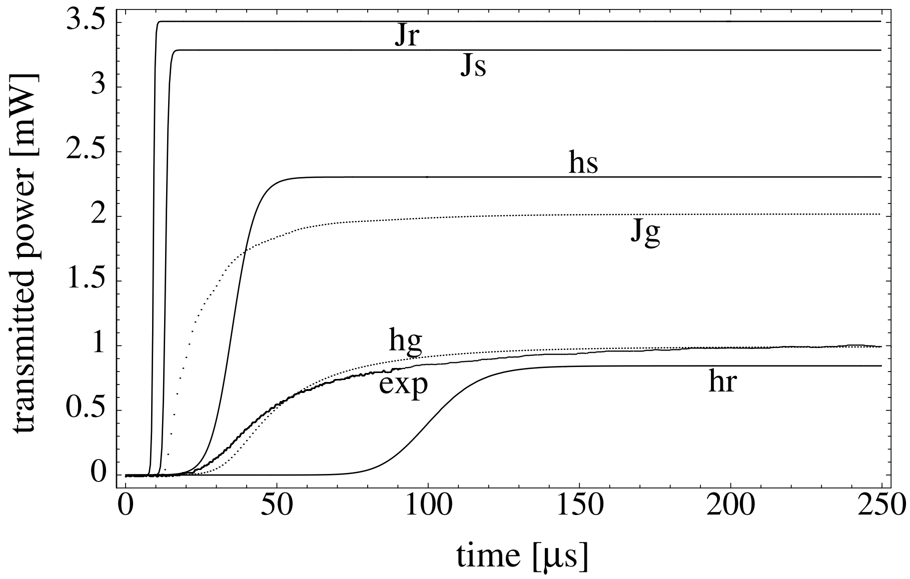

Figure 12.2: Transmitted power as a function of time after one circularly polarized beam is switched on at $t = 0$. Jr: $J = 1/2 \leftrightarrow J = 1/2$ rate model, Js: $J = 1/2 \leftrightarrow J = 1/2$ semiclassical model with plane wave, hs: hyperfine semiclassical model with plane wave, Jg: $J = 1/2 \leftrightarrow J = 1/2$ semiclassical model with gaussian input beam, hg: hyperfine semiclassical model with gaussian input beam, hr: hyperfine rate model, exp: experiment. No adjustable parameters were used, but the measured beam powers were corrected for cell window losses.

the HF model can be understood intuitively. Due to the increased number of states (fig.12.1(bottom)) one can imagine e.g. that the optical pumping process requires more time since an atom in the $m_F = -2$ ground state needs more pump cycles ("indirect" pumping) until it reaches the only pumped state $m_F = 2$. One can also imagine that pumped atoms which leave the beam interaction region contribute more strongly to the ground state magnetization decay rate than in the $J_{\frac{1}{2}}$ model where half of the in-drifting atoms are already in the pumped state compared to only $\frac{1}{8}$ in the case of the HF model. Besides the improvements with respect to the $J_{\frac{1}{2}}$ model the HF model also allows to address fundamentally new questions. Population trapping e.g. can be obtained if the energy splitting of the hyperfine levels is decreased. The HF model also allows for different relaxation and dephasing rates for each rank (0–4) in the irreducible tensor representation, giving a total of 14 relaxation constants compared to only 3 in the $J_{\frac{1}{2}}$ model. The HF model can in principle be extended to other atomic transitions and other alkali atoms or to the case of a two dimensional gas.

In the case of the semiclassical model -either in the $J = 1/2 \leftrightarrow J = 1/2$ approximation or with hyperfine structure- the resulting set of equations to be solved contains two hyperbolic partial differential equations (the wave equation for the two laser beam polarizations σ^+ and σ^-) of the form

$$\left[\left(\frac{\partial}{\partial z} + \frac{1}{c}\frac{\partial}{\partial t}\right) - \frac{ic}{2\omega}\left(\frac{\partial^2}{\partial x^2} + \frac{\partial^2}{\partial y^2}\right) \right] E_0^{\pm}(\vec{r}, t) = \frac{i\omega}{2c\epsilon_0} P_0^{\pm}(\vec{r}, t) \, . \tag{12.1}$$

coupled via the macroscopic polarization $P_0^{\pm}$ to the density matrix equations describing the sodium atoms. Since the common general libraries contain no satisfactory numerical procedures to solve such a system, we had to develop an algorithm ourselves. While solving the wave equation numerically, any discretization using a timestep Δt and a space step Δz in the propagation direction z the relation

$$\Delta t \leq \frac{\Delta z}{c} \tag{12.2}$$

must be observed in order not to violate causality. If we require a minimal resolution of, say, 20 steps in the z-direction inside our sodium cell, the resulting timestep will be $\Delta t = 10^{-11}$s at most. To simulate a typical experiment up to the stationary state at about 300μs we therefore need a minimum of 30 million timesteps. A program to calculate the beam pattern formation within the $J = 1/2 \leftrightarrow J = 1/2$-approximation in the steady state, written by Alan McCord[11], requires about 10 minutes to complete on our institute's server machine, a Sun-10. If we need the same time to calculate each time step for a dynamical calculation, it would therefore take about 500 years on the same machine, and about 10 times longer if we want to include the sodium hyperfine structure.

In numerics such a system is called extremely stiff. This means that the equations describing the laser beam which propagates at 300000 km/s, vary much faster than the equations describing the optical pumping which evolves at a timescale of several microseconds. Because of the following reasons the computing time can be reduced to about one day. First, our algorithm is more efficient than the one used for the steady state calculation. Second, it can be fully vectorized and parallelized. Third, it runs on a faster machine, the NEC SX-4 of the Centro Svizzero di Calculo Scientifico

(Swiss Scientific Computing Center, CSCS), for which it has been optimized. Fourth, a self develped routine to reduce the stiffness of the equations by a factor of up to 20 has been added.

When solving a stiff system, the fast timescale force the time step to be small even though for the slow timescale of the other equations it could be large. For a fast solution algorithm one therefore tries to decouple the equations in order to solve each equation with its appropriate timestep.

One dynamical 3-dimensional simulation results in about 1-2 GB of data which can then be processed into a video animation to display the time dependence of the various nonlinear effects. As an example of such a visualization, a wire bouncing simulation is shown in fig.12.3. This effect was first discovered by simulation, and

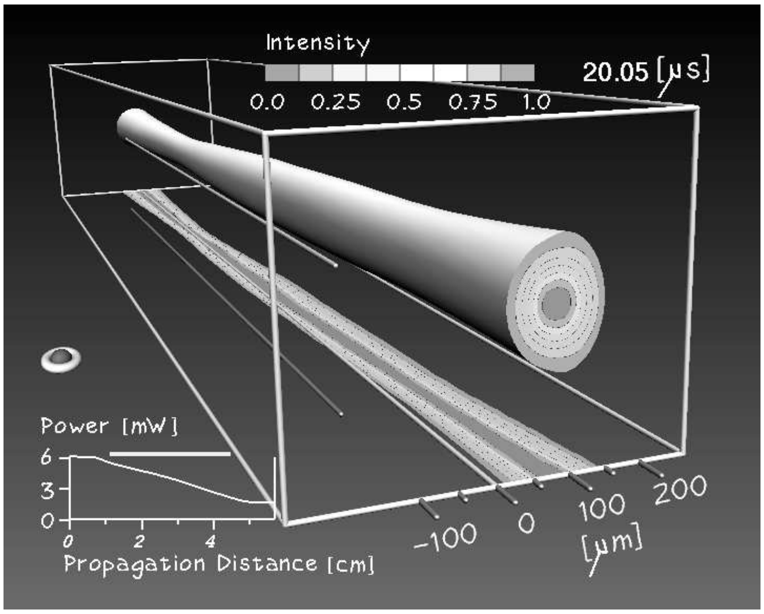

Figure 12.3: Still frame of a video animation done with data from a wire bouncing simulation. A current carrying wire deflects a circularly polarized laser beam by several beam widths, due to its inhomogeneous magnetic field. In this frame, the current has just been turned on for 0.05μs and the deflection is about 60μm.

later confirmed experimentally [6].

Both the Runge-Kutta step and the formulas to calculate the electrical field can be easily vector- and parallelized over the space variables. When also a vectorized/parallelized FFT is used, the total vectorization/parallelisation is nearly 100%. It has been very useful to implement all fields as one-dimensional, with running indices $i = 1 ... x_{end} \cdot y_{end} \cdot z_{end}$ in order to get large loops which can easily be optimized automatically. Also the fact that most laser beam setups are symmetric in the y-axis can be exploited to reduce the computing cost by almost 50%. On a NEC SX-3 we reach about 3 gigaflops (peak 6.4 GF) on one processor, while running in parallel on 8 CPU's of a NEC SX-4 (peak 16 GF) we obtain about 11.5 GF, regardless of the value of the stiffness factor s. The performance on the SX-4 scales almost proportionally with the number of processors used. As an example, the simulation of 60μs of "wire bouncing" with a spatial resolution of $60\times50\times27$ requires about 4 (wallclock-) hours in the $J=\frac{1}{2}$ to $J=\frac{1}{2}$ approximation and would require about 95 hours using the hyperfine density matrix equations, both on the SX-4.

The next goal will be to improve the experimental pattern detection techniques by using a fast CCD array. Theoretical studies will concentrate on how temporal and spatial fluctuations can influence the behavior of certain effects, e.g. if small fluctuations in the sodium vapor density can lead to the splitting of perfectly overlapping beams (or of one linearly polarized beam). Such fluctuations are easily integrated into the simulations, but difficult to control in the experiments. As an example, we show an Unstable configuration of two beams in Fig.12.4. The two beams of

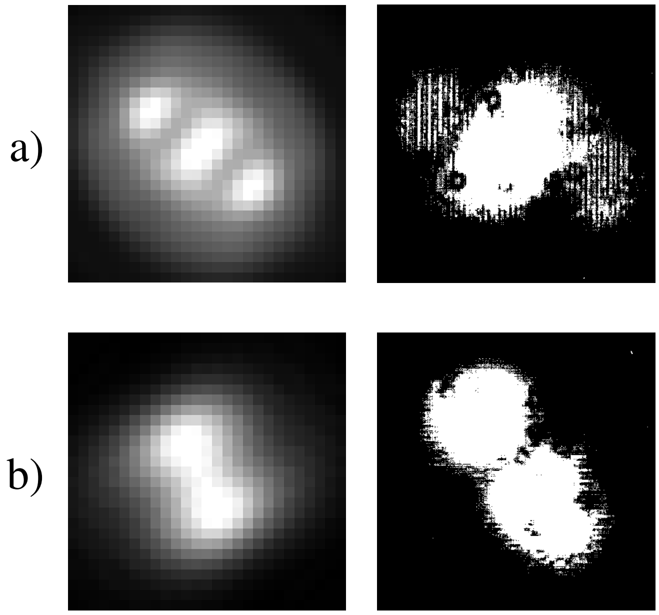

Figure 12.4: Fluctuating beams, in the experiment (right) and simulation (left), seen at the end of the cell. a) situation 1.23μs after the beams have been switched on, b) at 5.53μs. Unlike in the experiment, the simulation reaches a steady state after about 35μs, since no fluctuations have been built into the code. Parameters: sodium vapor temperature 255°C (atomic density $4.63\cdot10^{19}\mathrm{m}^{-3}$), cell length 6.5 cm, input power 25 mW per beam, beam waist 120μm at the cell input window, x-offset at input window 56μm, y-offset at input window 43μm, x-axis angle between beams 2.09 mrad, y-axis angle between beams 0.94 mrad, detuning 6.0 GHz, orientation decay rate in the lower level $\gamma_l = 1.6\cdot10^4\mathrm{s}^{-1}$, calculation grid size $72\times72\times43$.

opposite circular polarization are setup in a way that they only slightly touch each other inside the cell. While the beam patterns observed at the output window of the cell never stop fluctuating in the experiment, a steady state is reached in the calculation after about $35\mu s$ since no fluctuations have been added to the simulation. If, for example, one of the beam angles is changed slightly, a different steady state is reached. Apparently, fluctuations of the sodium vapor density, the laser intensity or the laser beam position and angle are sufficient to keep the system switching between different steady states. The understanding of such "chaotic" behavior might be the subject of future investigations.

References

[1] R. Holzner, J. Simonet, L. Flepp, B. Röhricht, P. Eschle, S. Dangel, U. Rusch, H. Schmid, and E. Brun. Using nuclear spins, radio waves, sodium atoms, and laser light to investigate spatiotemporal nonlinear systems. *Optical Engineering*, 34:2315–2323, 1995.

[2] R. Holzner, P. Eschle, A. W. McCord, and D. M. Warrington. Transverse "Bouncing" of Polarized Laser Beams in Sodium Vapor. *Phys.Rev.Lett.*, 69(15):2192–2195, 1992.

[3] S. Dangel, P. Eschle, B. Röhricht, U. Rusch, H. Schmid, and R. Holzner. Dynamics of laser beam switching in sodium vapor. *J. Opt. Soc. Am. B*, 12(4):681–686, 1995.

[4] B. Röhricht, A. W. McCord, M. Brambilla, F. Prati, S. Dangel, P. Eschle, and R. Holzner. Spatial separation of circularly polarized laser beams in sodium vapor. *Opt. Comm.*, 118:601–606, 1995.

[5] B. Röhricht, U. Rusch, S. Dangel, H. Schmid, P. Eschle, R. Holzner, and W.J. Sandle. Optical pumping induced ring structures of polarized laser light propagating through sodium vapor. *J. Opt. Soc. Am. B*, 12(8):1411–1415, 1995.

[6] R. Holzner, P. Eschle, S. Dangel, R. Richard, H. Schmid, U. Rusch, B. Röhricht, R. J. Ballagh, A. W. McCord, and W. J. Sandle. Observation of magnetic-field-induced laser beam deflection in sodium vapor. *Phys. Rev. Lett*, accepted for publication, 1997.

[7] R. Loudon. *The quantum theory of light.* Oxford University Press, Oxford, 1984.

[8] M. Ducloy. Nonlinear effects in optical pmping of atoms by a high-intensity multimode gas laser. general theory. *Phys. Rev. A*, 8(4):1844–1859, 1973.

[9] A. Omont. Irreducible components of the density matrix. *Prog. Quantum Electronics*, 5:69–138, 1977.

[10] U. Fano. Description of states in quantum mechanics by density matrix and operator techniques. *Rev. Mod. Phys.*, 29(1):74–93, 1957.

[11] A. W. McCord and R. J. Ballagh. Mutual beam reshaping by two interacting radiation modes. *J. Opt. Soc. Am. B*, 7(1):73–83, 1990.

[12] D. Suter. Optically excited Zeeman coherences in atomic ground states: nuclear-spin effects. *Phys.Rev.A*, 46(1):344–350, 1992.